PHYSICAL REVIEW C, VOLUME 62, 041301(R)

Superdeformed and highly deformed bands in ^{65}Zn and neutron-proton interactions in Zn isotopes

C.-H. Yu,[1] C. Baktash,[1] J. Dobaczewski,[2] J. A. Cameron,[3] M. Devlin,[4,*] J. Eberth,[5] A. Galindo-Uribarri,[1] D. S. Haslip,[3,†] D. R. LaFosse,[4,‡] T. J. Lampman,[3] I.-Y. Lee,[6] F. Lerma,[4] A. O. Macchiavelli,[6] S. D. Paul,[1,7] D. C. Radford,[1] D. Rudolph,[8] D. G. Sarantites,[4] C. E. Svensson,[3,6] J. C. Waddington,[3] and J. N. Wilson[5,§]

[1]*Physics Division, Oak Ridge National Laboratory, Oak Ridge, Tennessee 37831*

[2]*Institute of Theoretical Physics, Warsaw University, Hoza 69, PL-00681 Warsaw, Poland*

[3]*Department of Physics and Astronomy, McMaster University, Hamilton, Ontario, Canada L8S 4M1*

[4]*Chemistry Department, Washington University, St. Louis, Missouri 63130*

[5]*Institut für Kernphysik, Universität zu Köln, D-50937 Köln, Germany*

[6]*Nuclear Science Division, Lawrence Berkeley National Laboratory, Berkeley, California 94720*

[7]*Oak Ridge Institute for Science and Education, Oak Ridge, Tennessee 37831*

[8]*Department of Physics, Lund University, S-22100 Lund, Sweden*

(Received 31 May 2000; published 11 September 2000)

Superdeformed and highly deformed rotational bands were established in ^{65}Zn using the ^{40}Ca(^{29}Si,$4p$)^{65}Zn reaction, and averaged quadrupole moments were measured for two of these bands. The configurations of these bands were assigned based on Hartree-Fock calculations. One of the three bands exhibits at low $\hbar\omega$ a rise in the $J^{(2)}$ dynamic moments of inertia that is similar to the alignment gain observed in ^{60}Zn. A comparison of the rotational band configurations and their $J^{(2)}$ moments of inertia for light Zn isotopes suggests that the rise in $J^{(2)}$ is most likely caused by np interactions associated with the valence protons and neutrons occupying the $g_{9/2}$ intruder orbits.

PACS number(s): 21.10.Re, 21.10.Hw, 23.20.Lv, 27.50.+e

Recent studies [1–6] of superdeformed (SD) and highly deformed bands in $^{60-64,68}$Zn have allowed systematic analyses of strongly deformed shapes and configurations in nuclei with $N \approx Z$. In the previous study [1] of ^{60}Zn, a rise in the $J^{(2)}$ moments of inertia of the SD band was interpreted as the simultaneous alignment of the $g_{9/2}$ protons and neutrons. However, the absence of such an alignment in the SD band of ^{61}Zn raises questions [2] of whether or not the $T=0$ pairing is responsible for such an alignment. To understand the true cause of the rise in $J^{(2)}$, and to gain insight into the questions of the possible $T=0$ pairing, more experimental data are needed for the neighboring nuclei. In this paper, we report a study of SD and highly deformed bands in ^{65}Zn, and present possible evidence for neutron-proton correlations in highly-deformed Zn isotopes.

High spin states in ^{65}Zn were populated using the ^{40}Ca(^{29}Si,$4p$) reaction at a beam energy of 130 MeV. The ^{29}Si beam was provided by the 88-Inch Cyclotron at the Lawrence Berkeley National Laboratory, and the target consisted of a layer of 0.5 mg/cm^2 enriched ^{40}Ca evaporated onto a layer of 2.5 mg/cm^2 Ta foil as backing. The γ rays from the reaction were detected by the Gammasphere [7] array, which had 100 detectors at the time of the experiment. The evaporated charged particles were detected by the 95-element CsI detector array Microball [8], and the information obtained was used to select the reaction channel, as well as to determine the velocity of the recoil for event-by-event Doppler corrections. A total of about 88 million 4-proton gated $\gamma\gamma\gamma$ or higher fold events were collected from the experiment. Three rotational bands were established from the reaction-channel-selected $\gamma\gamma\gamma$ cube, and are shown in Fig. 1. Although no connecting transitions were observed between these bands and the low-spin normally deformed (ND) states [9] in ^{65}Zn, they are assigned to ^{65}Zn with confidence due to their unambiguous coincidence relationships with the known [9] transitions in ^{65}Zn (see Fig. 2).

Among the three established bands, band 1 is the most strongly populated and is measured to have the largest deformation (see ensuing discussions on measurement of Q_t's). The average intensity of this band is approximately 2.5% of that of the 202-keV ND transition at low spin (see Fig. 3). A spectrum obtained by summing all possible double gates in this band is strongly in coincidence with the 202-, 864-, 987-, and 1173-keV ND transitions in ^{65}Zn, as seen in Fig. 2(a). For this spectrum, the $\gamma\gamma\gamma$ cube has Doppler corrections performed at two different recoil velocities: For $E_\gamma > 1350$ keV, $v_{\rm rec}/c = 0.04$, which corresponds to fast decays of SD bands; for $E_\gamma < 1350$ keV, $v_{\rm rec}/c = 0.027$, which corresponds to decays of low spin states occurring when the recoil has been slowed down by the backing and is traveling in vacuum. As a result of this dual-velocity Doppler correction, Fig. 2(a) shows narrow peaks for both the SD band as well as the low spin ND transitions. The spectrum obtained by summing all possible combinations of double gates on

*Present address: LANSCE-3, MS H855, Los Alamos National Laboratory, Los Alamos, NM 87545.

†Present address: Defence Research Establishment Ottawa, Ottawa, Ontario, Canada.

‡Present address: Department of Physics, State University of New York at Stony Brook, Stony Brook, NY 11794.

§Present address: Niels Bohr Institute, Blegdamsvej 17, DK-2100 Copenhagen Ø, Denmark.

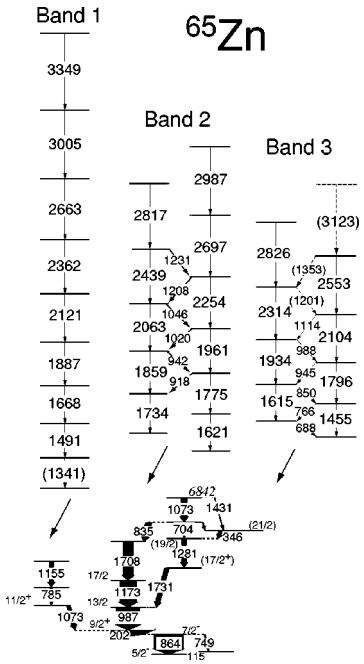

FIG. 1. Level scheme of the three rotational bands and some ND transitions in ^{65}Zn established in the present study. Spins and parities are adopted from Ref. [9].

$M1$ and $E2$ transitions in band 2, as well as double gates between the 202-keV transition and members of band 2 are shown in Fig. 2(b). Coincidence gates show weak, but definite connections between the two signatures of this band. The intensity of this band is about one half of that of band 1, as shown in Fig. 3(a). Band 3 is a strongly coupled band and Fig. 2(c) shows the spectrum of this band obtained in a manner similar to that described for band 2. For spectra shown in Figs. 2(b) and 2(c), the Doppler effect was corrected with one velocity only: $v_{\mathrm{rec}}/c=0.04$. This is to accommodate the lower-energy, fast $M1$ transitions in bands 2 and 3. As a result, the low spin ND transitions at 864, 988, and 1173 keV are broadened due to the overcorrection of the Doppler effect. Because of the low statistics, only the average relative intensity of band 3 was estimated, which is approximately 0.7% of that of the 202-keV ND transition [see Fig. 3(a)].

In order to extract information on γ ray multipolarities, data were summed up from the 23 most forward and backward detectors (at 31.7°, 37.4°, 142.6°, 148.3°, and 162.7°), and the 22 detectors near 90° (at 79.2°, 80.7°, 90°, 99.3°, and 100.8°) to form two groups labeled as ''32°'' and ''81°,'' respectively. (The labels represent the effective angles corresponding to the averaged cosines of the two detector groups.) A 32°-versus-all and an 81°-versus-all matrix were created. From these two matrices, information of angular distribution was obtained by extracting ratios defined as

$$\frac{I(32°)}{I(81°)}(\gamma_1)=\frac{I(\gamma_1 \text{ at } 32°, \text{ gated with } \gamma_2 \text{ at any } \theta)}{I(\gamma_1 \text{ at } 81°, \text{ gated with } \gamma_2 \text{ at any } \theta)}. \quad (1)$$

Figure 3(b) shows these gated angular distribution (GAD) ratios for clean, strong transitions in band 1 and band 2, as

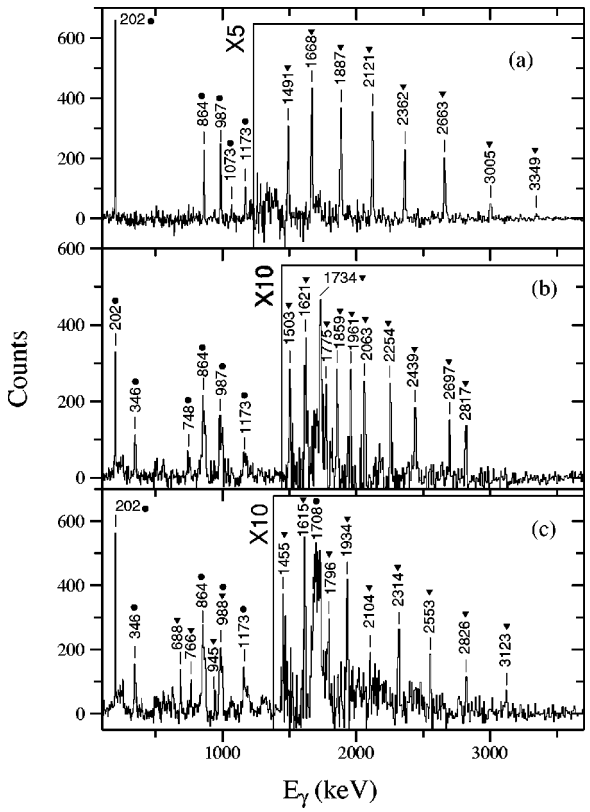

FIG. 2. Coincidence spectra representing the three bands in ^{65}Zn. Triangles indicate members of the bands and circles indicate the low spin ND transitions. See text for details of the Doppler correction. (a) Spectrum obtained by summing all possible double gates in the SD band 1. (b) Spectrum obtained by summing all double gates on band 2, as well as double gates between the 202-keV ND transition and members of band 2. (c) Spectrum obtained by summing all double gates on band 3, as well as double gates between the 202-keV ND transition and members of band 3.

well as for some ND dipole (diamond) and quadrupole (square) transitions at low spin. No GAD ratio could be extracted for band 3 due to low statistics. Compared to the ND transitions with known multipolarities, the GAD ratios for transitions in band 1 and band 2 confirm the multipolarity

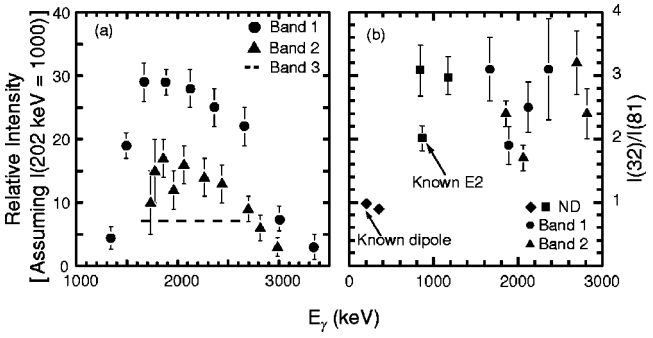

FIG. 3. (a) Intensities of the three bands in ^{65}Zn measured relative to that of the 202-keV ND transition at low spin. (b) Gated angular distribution (GAD) ratios measured for clean, strong transitions in bands 1 and 2, and compared to those of the known [9] $E2$ and dipole ND transitions at low spin.

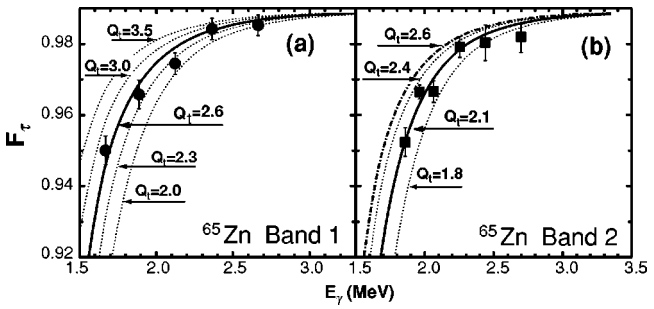

FIG. 4. Experimental (filled symbols) and calculated (curves) values of F_τ as a function of E_γ for (a) SD band 1 and (b) band 2. See text for details of the measurement and calculation.

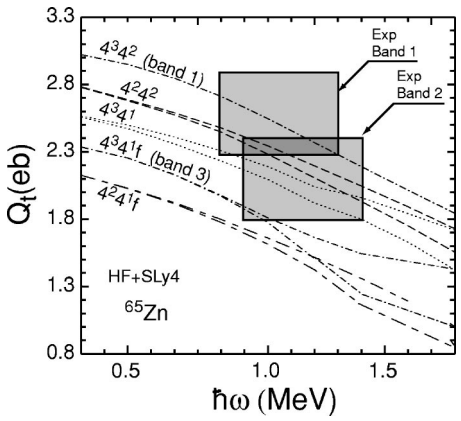

FIG. 5. Calculated (HF+SLy4) Q_t's as a function of $\hbar\omega$ for possible configurations in ^{65}Zn. The shaded areas represent the measured, average Q_t's for band 1 and band 2.

assignments shown in Fig. 1. For band 3, the strong $M1$ transitions connecting the two signatures indirectly support the assigned multipolarities.

Since no linking transitions were established between the observed three bands and the low spin ND states, the spins and excitation energies of these bands could not be deduced. Coincidence relationships show that for band 1, the highest ND level with which the band is in coincidence is the 6842-keV level. This means that the spin of the final level of the 1341-keV transition in this band has a lower limit of $I \geqslant 25/2$, which is consistent with the established [1,2] spins of the SD bands in ^{60,61}Zn.

The average transition quadrupole moments, Q_t, were measured for band 1 and band 2. Using the technique described in Refs. [10,11], the relative velocity of the recoils, $F_\tau = v(E_\gamma)/v_{\max}$, were extracted and shown in Fig. 4 together with calculations [$v(E_\gamma)$ is the recoil velocity at the time when E_γ is emitted, and $v_{\max}$ is the maximum recoil velocity for the $4p$ reaction channel]. The calculations used the LINESHAPE program [12] and the stopping powers in Ref. [13] (corrected according to Ref. [14]). The simulations used a time step of 0.7 fs and produced 1000 histories. Side feedings were modeled by a two-level rotational sequence into each state with the same Q_t and $J^{(2)}$ as the band. The uncertainty associated with these assumptions is not included in the final results, but is expected to be much smaller than the shown errors. Additional errors associated with stopping powers could not be estimated from the present study. The best fit between the experimental and calculated F_τ's resulted in a $Q_t = 2.6 \pm 0.3\ e$ b for band 1, and $Q_t = 2.1 \pm 0.3\ e$ b for band 2 [see Figs. 4(a) and 4(b), respectively]. Assuming an axially symmetric shape, this corresponds to a deformation of $\beta_2 = 0.43 \pm 0.05$ and 0.35 ± 0.05 for band 1 and band 2, respectively. These measured Q_t's are compared to calculations in Fig. 5. Quadrupole moment was not measured for band 3 due to low statistics.

Theoretical analysis of the SD bands in ^{65}Zn has been performed using the HF method (no pairing, code HFODD v1.75 [15]) with the Skyrme SLy4 interaction [16]. As discussed in Refs. [17,18], configurations of the SD nuclei in the $A \simeq 60$ region can be characterized by n and p occupied neutron and proton $g_{9/2}$ $\mathcal{N}=4$ intruder states, and are denoted by $4^n 4^p$. Neutron and proton single-particle Routhians, calculated for the $4^3 4^2$ configuration of ^{65}Zn, show that at large rotational frequencies ($\hbar\omega$), energy gaps open up at $N=35$ and $Z=30$ for neutrons and protons, respectively. Therefore, the positive-parity $4^3 4^2$ configuration is expected to be yrast at high angular momenta, and will be referred to as the magic SD configuration in the following discussion.

The last neutron in ^{65}Zn occupies the third $\mathcal{N}=4$ intruder state, denoted by the Nilsson labels [431]3/2 ($r=-i$, or $\alpha = +1/2$), where $r = e^{-i\alpha\pi}$ is the signature quantum number, and α is the signature index. In the following discussion, the single-particle states (or many-body configuration $4^n 4^p$) are labeled by signs ($\pm$) denoting the single-particle (or many-body configuration total) signature indices $\alpha = \pm 1/2$. Therefore symbol ($+$) refers to bands with spins 25/2, 29/2, . . . , and ($-$) refers to those with spins 27/2, 31/2, ... Note that the magic configuration $4^3 4^2(+)$ corresponds to $\alpha = +1/2$.

The lowest unoccupied neutron states are the fourth intruder state [431]3/2($-$) at low spins, and the pair of signature-split [312]3/2 states at high spins. The last occupied proton state in ^{65}Zn corresponds to the second intruder orbital [440]1/2($-$), and two pairs of negative-parity orbitals are available for proton excitations, i.e., the [303]7/2($\pm$) and [310]1/2($\pm$) orbitals. Altogether, there are three neutron and four proton low-lying one-particle-hole excitations in ^{65}Zn. Calculations show that the magic $4^3 4^2$ configuration is yrast at high spins, but is crossed at $I \simeq 53/2$ by the pair of negative-parity signature-degenerate configurations $4^3 4^1 f(\pm)$, which are formed by exciting the [440]1/2($-$) proton to the [303]7/2($\mp$) negative-parity states. (Configurations corresponding to the occupation of one $K=7/2$ $f_{7/2}$ proton extruder states are denoted by adding f to symbol $4^n 4^p$.) Three additional pairs of coupled bands are also near the magic $4^3 4^2$ configuration: (i) negative-parity bands $4^3 4^1(\pm)$ correspond to promoting the [440]1/2($-$) proton to the [310]1/2($\mp$) states, (ii) negative-parity bands $4^2 4^2(\pm)$ correspond to promoting the [431]3/2($+$) neutron to the [312]3/2($\pm$) states, and (iii) positive-parity bands $4^2 4^1 f(\pm)$ correspond to promoting the [431]3/2($+$) neutron to the [312]3/2($-$) state and simultaneously promoting the [440]1/2($-$) proton to one of the [303]7/2($\pm$) states.

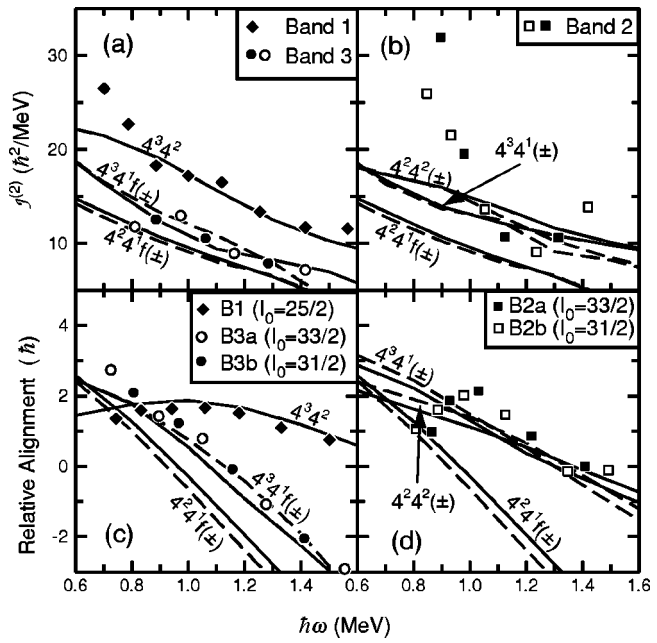

FIG. 6. (a) and (b): Calculated (curves) and experimental (symbols) $J^{(2)}$ moments of inertia for bands observed in ^{65}Zn. (c) and (d): Calculated (curves) and experimental (symbols) alignments relative to that of the SD band in ^{61}Zn for bands observed in ^{65}Zn. I_0 represents the tentatively measured (I_0=25/2 for ^{61}Zn [2]) or assumed (all other bands) spins of the lowest levels of the bands. Solid and dashed curves represent the ($\alpha=+1/2$) and ($\alpha=-1/2$) signatures, respectively.

In the following, we first discuss the experimentally observed bands 1 and 3 in ^{65}Zn. Figure 6(a) shows the calculated (curves) and experimental (symbols) $J^{(2)}$ dynamic moments of inertia for band 1 and band 3 in ^{65}Zn. This figure shows that the magic $4^3 4^2(+)$ and the $4^3 4^1 f(\pm)$ configurations nicely reproduce the experimental data for bands 1 and 3, respectively. When the lowest spins for these two bands are assumed to be 25/2 and 31/2, respectively, and when adopting the tentatively measured [2] lowest spin of $I_0=25/2$ for the SD band in ^{61}Zn, the calculated relative alignments for these two configurations also reproduce the experimental data very well [see Fig. 6(c)]. Such a good agreement suggests strongly that the observed band 1 is the magic $4^3 4^2$ configuration, and band 3 is the $4^3 4^1 f$ configuration. For band 1, the measured average Q_t also agrees nicely with the predicted Q_t's for the magic $4^3 4^2$ configuration [see Fig. 5].

Theoretical interpretation of band 2 is much more difficult. In addition to the $4^3 4^1 f(\pm)$ configuration that is already assigned to band 3, there are three other possible configurations for excited bands in ^{65}Zn, i.e., the $4^2 4^1 f(\pm)$, $4^3 4^1(\pm)$, and $4^2 4^2(\pm)$ configurations. The comparison of measured and calculated Q_t's for band 2 essentially eliminates the possibility of the $4^2 4^1 f(\pm)$ configuration, as shown in Fig. 5. When the lowest spin is assumed to be $I_0=31/2$, the calculated relative alignments for the negative-parity $4^3 4^1(\pm)$ and $4^2 4^2(\pm)$ configurations qualitatively agree with data, see Fig. 6(d). Furthermore, the measured Q_t's for band 2 also qualitatively agree with the calculated

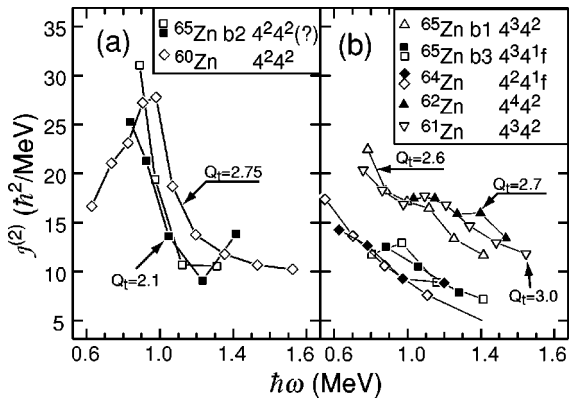

FIG. 7. Experimental $J^{(2)}$ moments of inertia for SD and highly deformed bands observed in $^{60-65}$Zn. The bands are grouped into (a) those with a rise in $J^{(2)}$, and (b) those without such a rise. See text and Refs. [1–3,5,19] for the indicated configurations $4^n 4^p$. The question mark for band 2 of ^{65}Zn in (a) indicates that this configuration assignment is tentative.

ones for the $4^3 4^1(\pm)$ and $4^2 4^2(\pm)$ configurations (see Fig. 5). Since the observed energy signature splitting in band 2 is small, and since the $4^2 4^2(\pm)$ configuration has a smaller signature splitting than the $4^3 4^1(\pm)$ configuration, we tentatively assign the $4^2 4^2(\pm)$ configuration to band 2.

The rise in the $J^{(2)}$ dynamic moments of inertia at low spin in band 2 cannot be reproduced by calculations of any configuration [see Fig. 6(b)]. This rise could be due to the alignment of neutrons or protons associated with the normal neutron-neutron (nn), proton-proton (pp), or some type of neutron-proton (np) pairing, none of which is included in the present calculations. Indeed, a rise in the $J^{(2)}$ dynamic moments of inertia has been observed [1] in the SD band of ^{60}Zn, and has been interpreted as the simultaneous alignment of the $g_{9/2}$ protons and neutrons. Figure 7(a) shows the $J^{(2)}$'s for the ^{60}Zn band compared to those of band 2 in ^{65}Zn. The similarity of these two bands is clearly seen.

Also summarized in Fig. 7 are the assigned configurations for bands observed in light Zn isotopes and their $J^{(2)}$ dynamic moments of inertia. For bands observed in $^{60-65}$Zn, those with a rise in $J^{(2)}$ are plotted in Fig. 7(a), and all other smooth bands are plotted in Fig. 7(b). The absence of the rise in bands shown in Fig. 7(b) cannot be understood in terms of the ''blocking'' of odd valence particles. If the rise in $J^{(2)}$ is caused by the simultaneous alignment of $g_{9/2}$ protons and neutrons associated with the normal nn and pp pairing alone, then the occupation of an odd number of $g_{9/2}$ protons (neutrons) should only block the proton (neutron) part of the alignment. As a result, the $J^{(2)}$ should show a reduced, but nonvanishing rise in configurations such as $4^3 4^2$ and $4^2 4^1 f$. Figure 7 shows, however, that the occupation of one odd particle (protons or neutrons) is as effective as the occupation of both an odd proton and an odd neutron in blocking the entire alignment. (Note that the ^{62}Zn band does not have sufficient data at low spin where the alignment is observed, and therefore cannot be firmly characterized as a ''smooth'' band.) The absence of the rise in $J^{(2)}$ shown Fig. 7(b) is also unlikely to be caused by deformation differences. If the alignment is shifted up or down in frequency due to larger or

smaller (or vice versa) deformations, and thus is outside the experimentally observed data region, then the smooth bands must have a very different deformation compared to bands that show the rise. The measured Q_t's indicated in Fig. 7 show that this is not the case. Bands with both large ($Q_t \simeq 2.6-3.0\ e$ b) and small ($Q_t \simeq 2.0\ e$ b) deformations are associated with both rising and smooth $J^{(2)}$'s. [Experimental Q_t's for the ^{64}Zn band and band 3 in ^{65}Zn are not available. However, they are expected to be small, judging by their configurations and their relatively low $J^{(2)}$'s.]

Further analysis show that the rise in $J^{(2)}$ may be correlated with configurations. In Fig. 7(a), the two bands showing the rise most likely share a configuration that is quite unique among all bands. If band 2 of ^{65}Zn indeed has the $4^2 4^2$ configuration, then the two bands shown in Fig. 7(a) both have two neutrons occupying the lowest two $g_{9/2}$ orbits, and two protons occupying the exact same orbits. In other words, their occupation of the $g_{9/2}$ intruder orbits are *identical* for valence protons and neutrons (can be labeled as a $4^m 4^m$ configuration, where $m=n=p$ in the previously defined notation $4^n 4^p$). Among all the observed bands in $A=60$ region, the two bands shown in Fig. 7(a) are the only ones which have been assigned (firmly or tentatively) $4^m 4^m$ configurations, and they are also the only bands which show a definite rise in $J^{(2)}$. If such a correlation is not a coincidence, then this implies that (1) the interaction that is responsible for the observed alignment is most likely np, instead of pp or nn, in nature; (2) such an np interaction exists only when the occupation of high-j intruder states is identical for protons and neutrons.

In summary, one SD and two highly deformed bands in ^{65}Zn were established from a Gammasphere experiment. Configurations of two of the three bands were unambiguously assigned based on Hartree-Fock calculations. One of the three bands shows a rise in $J^{(2)}$ at low spins, which is similar to the rise observed [1] in ^{60}Zn, and cannot be explained within the Hartree-Fock calculations without pairing. A systematic analysis of the $J^{(2)}$ values for bands in $^{60-65}$Zn indicates that the normal nn, pp pairing alone cannot be the only cause for the observed alignment. np interactions are most likely the main cause for the rise, and such interactions appear to exist only when the coccupation of the $g_{9/2}$ intruder states is identical for valence protons and neutrons.

Oak Ridge National Laboratory is managed by UT-Battelle, LLC, for the U.S. D.O.E under Contract No. DE-AC05-00OR22725. This work was also supported by the U.S. D.O.E [Contracts No. DE-AC05-76OR00033 (ORISE) and No. DE-FG05-88ER40406 (WU)], the Polish CSR (Contract No. 2 P03B 040 14), the Natural Science and Engineering Research Council of Canada, and the Swedish Natural Science Research Councils.

[1] C.E. Svensson *et al.*, Phys. Rev. Lett. **82**, 3400 (1999).
[2] C.-H. Yu *et al.*, Phys. Rev. C **60**, 031305 (1999).
[3] C.E. Svensson *et al.*, Phys. Rev. Lett. **79**, 1233 (1997).
[4] S.D. Paul *et al.*, in Proceedings of Nuclear Structure '98, Gatlinburg, Tennessee, 1998, Book of Abstracts, p. 100.
[5] A. Galindo-Uribarri *et al.*, Phys. Lett. B **422**, 45 (1998).
[6] M. Devlin *et al.*, Phys. Rev. Lett. **82**, 5217 (1999).
[7] I.Y. Lee, Nucl. Phys. **A520**, 641c (1990).
[8] D.G. Sarantites *et al.*, Nucl. Instrum. Methods Phys. Res. A **381**, 418 (1996).
[9] G.F. Neal *et al.*, Nucl. Phys. **A295**, 351 (1978).
[10] B. Cederwall *et al.*, Nucl. Instrum. Methods Phys. Res. A **354**, 591 (1995).
[11] C.-H. Yu *et al.*, Phys. Rev. C **57**, 113 (1998).
[12] J.C. Wells *et al.*, ''LINESHAPE: A Computer Program for Doppler Broadened Lineshape Analysis,'' ORNL Physics Division Prog. Rep. 30, 1991, No. ORNL-6689.
[13] L.C. Northcliffe and R.F. Schilling, Nucl. Data Tables **7**, 233 (1970).
[14] J.F. Ziegler and W.K. Chu, At. Data Nucl. Data Tables **13**, 463 (1974).
[15] J. Dobaczewski and J. Dudek, Comput. Phys. Commun. **102**, 166 (1997); **102**, 183 (1997); nucl-th/0003003.
[16] E. Chabanat *et al.*, Nucl. Phys. **A635**, 231 (1998).
[17] D. Rudolph *et al.*, Phys. Rev. Lett. **80**, 3018 (1998).
[18] J. Dobaczewski, W. Satuła, W. Nazarewicz, and C. Baktash (unpublished).
[19] A.V. Afanasjev, I. Ragnarsson, and P. Ring, Phys. Rev. C **59**, 3166 (1999).